Cent. Eur. J. Phys.
DOI: 10.2478/s11534-008-0135-9

VERSITA

Central European Journal of **Physics**

Ionization effects and linear stability in a coaxial plasma device

Research Article

Erol Kurt[1]*, Hilal Kurt[2], Ulku Bayhan[3]

1 *Department of Electrical Education, Faculty of Technical Education, Gazi University, 06500 Besevler, Ankara, Turkey*

2 *Department of Physics, Faculty of Arts and Sciences, Gazi University, 06500 Besevler, Ankara, Turkey*

3 *Department of Physics, Faculty of Arts and Sciences, Mehmet Akif Ersoy University, 15030 Yenimahalle, Burdur, Turkey*

Received 14 May 2008; accepted 9 October 2008

Abstract: A 2-D computer simulation of a coaxial plasma device depending on the conservation equations of electrons, ions and excited atoms together with the Poisson equation for a plasma gun is carried out. Some characteristics of the plasma focus device (PF) such as critical wave numbers a_c and voltages U_c in the cases of various pressures P are estimated in order to satisfy the necessary conditions of traveling particle densities (*i.e.* plasma patterns) via a linear analysis. Oscillatory solutions are characterized by a nonzero imaginary part of the growth rate $\Im(\sigma)$ for all cases. The model also predicts the minimal voltage ranges of the system for certain pressure intervals.

PACS (2008): 03.65.Db, 03.65.Ge

Keywords: coaxial plasma device • oscillatory instability • ionization

1. Introduction

A plasma focus (PF) device is one of the well-known devices known as plasma guns, which consists of one anode and several cathode bars surrounding it in a cylindrical geometry [1, 2]. When the spark gap is activated, a capacitor with a series connection to the PF provides a sufficient electrical energy in order to initiate a breakdown between the anode and cathode space under a suitable gas pressure. The dynamics of a PF consists mainly of three individual phases just after the electrical current starts to pass through the spark gap. Among them the initial phase is responsible for the breakdown and the first formation of the current sheath just above the insulator on the central electrode [2–4]. The second one is the acceleration phase which pushes the sheath towards the open end of anode by the Lorentz force [5]. The last phase of the discharge is the collapse of the current sheaths in front of the anode tip [2, 6]. Yields such as neutrons, charged particles and ions as well as intense radiation are emitted in this last stage [1].

Previous studies have shown that pinch formulation and

*E-mail: ekurt52tr@yahoo.com

the corresponding plasma acceleration are strongly related to the initial stages of discharges [7–9]. An optimal PF operation and maximal yield depend on previous plasma stages of a focus. Thus, perfect determination of the initial stages of the plasma dynamics is important for the estimation of optimal working conditions. In this framework, the question "whether the pressure and the critical breakdown voltage are in the optimal ranges" comes to the forefront. At this point, the aim should be the identification of plasma patterns as functions of the aforementioned system parameters. The plasma stability, namely, the linear stability analysis, which sketches out a criterion on the formation of the potential and the islands of electrons, ions and excited atoms between the electrodes plays an important role. In addition, the plasma may show some different characters due to stability conditions. Frequently, a sudden onset, burst of energy, momentum and particles across magnetic surfaces and an avalanche character are observed in different variations of the system parameters.

In order to enhance the efficiency of the yields in PF devices, a number of studies have been realized by focusing on the different physical properties of the devices; for instance the insulator length, insulating material, and distances between the electrodes [7, 8, 10]. In addition to those researches, there also exist different *mhd* modeling studies in the literature [4, 11–13]. However, the aforementioned studies did not handle the linear stability analysis which describes the required system parameters for the formation of plasma sheath inside the inter-electrode area in terms of so-called Paschen curves. Another important motivation in this paper is as follows: PF experiments have shown that there exist a certain mass loss in the inter-electrode region during the axial phase. In a typical experiment, at least $20-40\%$ of the initial mass of the current sheath which is generated in the breakdown phase is lost [14–16]. In other words, a certain number of electrons and ions always escape from the spaces between the cathode rods while the plasma sheath moves. In order to compensate the losses of ions and electrons, one has to accept a continuous ionization process which covers also the axial phase. Otherwise the system can not lead to higher particle densities due to the insufficient numbers of electrons and ions. This reality forces us to use the mechanism of breakdown in the axial phase. In other words, ionization and diffusion mechanisms should also be applied to the axial phase as in the breakdown phase [17]. The voltage drop in the breakdown phase, which generally occurs for 100-500 nanoseconds in real focus experiments is considered to be very low, so one can also use the initial voltage value U for the axial phase. In the light of these preliminary initial ideas, a linear stability analysis

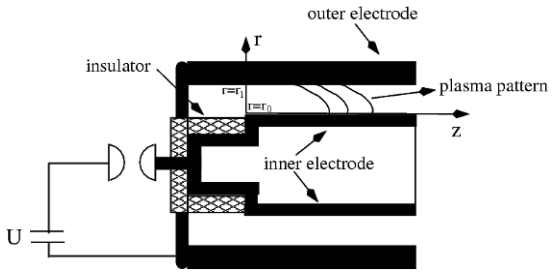

Figure 1. Schematic representation of a plasma focus system. Plasma pattern moves through the tip of electrodes in the axial phase.

is carried out to construct the threshold in PF devices in the axial phase. To our knowledge, there exists no sufficient stability analysis in the literature for PF devices. The analysis is realized via a computer simulation of the plasma patterns at the acceleration phase in the coaxial electrode system Fig. 1. In the model, we only use the basic concepts of conservation equations for electrons, ions and excited atoms.

2. Theoretical description of problem

Initially, we assume a coaxial electrode system as in Fig. 1. When the spark gap is short-cut, a current flows through the electrodes from the capacitor bank, which has a voltage U. After the breakdown phase which occurs just above the insulator sleeve on the anode, the current sheath moves into the inter-electrode space to the right of the radial axis "r". The plasma dynamics basically in this area is considered for the numerical simulation and the lower and upper boundaries are assumed to be "$r = r_0$" and "$r = r_1$" for the numerical process.
From a theoretical point of view, we consider the particle conservation equations for electrons, ions and excited atoms. In this manner, the corresponding equations can be written as follows:

$$\begin{aligned} \frac{\partial N_e}{\partial t} + \nabla \cdot (N_e \vec{u_e}) &= Q_e^+ + Q_e^- + D_e \nabla^2 N_e, \\ \frac{\partial N_i}{\partial t} + \nabla \cdot (N_i \vec{u_i}) &= Q_i^+ + Q_i^- + D_i \nabla^2 N_i, \\ \frac{\partial N_a}{\partial t} &= Q_a^+ + Q_a^- + D_a \nabla^2 N_a. \end{aligned} \qquad (1)$$

Here, N indicates the number density of corresponding particles, and $\vec{u}$ gives the drift velocity. D is the diffusion coefficient and it is frequently considered as unity (i.e $D = 1$) in this analysis since diffusion term is assumed

to contribute the dynamics effectively. Moreover different D values can easily be adopted to the model depending on gas media. In the case of produced and lost particles per unit volume, Q^+ and Q^- are used respectively. There exist various forms for source terms in literature. Since we consider the plasma pattern as a complex and nonlinear structure, Q^+ and Q^- can be determined as αN and $-1/3\beta N^3$ (see in [18, 19]). Meanwhile we only deal with the linear analysis in this study, we do not take into account the term Q^-, which includes a higher order of N. The subscripts e, i and a refer to electrons, ions and excited atoms respectively. The conservation equations (1) are coupled with the Poisson equation,

$$\nabla^2\phi = \frac{4\pi}{\varepsilon} e(N_i - N_e), \tag{2}$$

which gives the relation between the particle densities and the electrical potential function.
According to the linear stability analysis, the task is first to find out the threshold values which satisfy the following expressions:

$$\begin{aligned} \mathcal{C}\frac{d}{dt}V(\vec{x},t) &= \mathcal{L}V(\vec{x},t), \\ \mathcal{L} &= \mathcal{A} + \alpha(U,P)\cdot\mathcal{B}, \end{aligned} \tag{3}$$

where the symbolic vector $V(\vec{x},t) = (N) = (N_e, N_i, N_a)$ represents the quantities in Equations (1-2). Moreover, $\vec{V}(\vec{x},t) \equiv 0$ corresponds to the ground state including space and time dimensions. The operators $\mathcal{C}$, $\mathcal{L}$, $\mathcal{A}$ and $\mathcal{B}$ are linear differential operators. We have the quantity $\alpha(U,P)$ in Eq. (3) for the explicit form of the linear operator $\mathcal{L}$ and it will be described later in detail. For now, we only state that α is an empirical quantity which is a function of voltage U and filling gas pressure P. Ionization mostly occurs near the electrodes. In this sense, the particle densities can be taken as unity at the boundaries. In the case of the electrical potential, a finite potential exists at the boundaries due to the voltage difference between the electrodes. In the light of this information, the following boundary conditions can be stated:

$$\begin{aligned} N = 1 \quad &\text{and} \quad \tfrac{\partial N}{\partial r} = 0 \quad \text{at} \quad r = r_0 \quad \text{and} \quad r = r_1, \\ \phi = \phi_0 = U \quad &\text{at} \quad r = r_0 \quad \text{and} \quad \phi = 0 \quad \text{at} \quad r = r_1. \end{aligned} \tag{4}$$

The solution ansatz the for density functions and potential can be given as,

$$\begin{aligned} V(\vec{x},t) = V(r,z,t) &= \tilde{V}(r)e^{(iaz+\sigma t)} \\ &= \tilde{V}(r)e^{i(az+\Im(\sigma)t)}e^{\Re(\sigma)t}, \\ \phi(\vec{x}) = \phi(r,z) &= \tilde{\phi}(r)e^{i(az+\Im(\sigma)t)}e^{\Re(\sigma)t}, \end{aligned} \tag{5}$$

where $\tilde{V}(r)$ is the general form for the functions $\tilde{N}_e(r)$, $\tilde{N}_i(r)$, $\tilde{N}_a(r)$. The functions are solved numerically through the fourth order Runge-Kutta shooting method subject to the boundary conditions given in Eq. (4). From the numerical point, effective computer routines are available in order to solve this eigenvalue problem (see in [20]). In Eq. (5), the quantity "a" in the exponential expression is nothing other than the wave number of the inter-electrode plasma pattern along the "z" direction. The growth rate is indicated by σ in the time dimension. After putting the ansatz (Eq. (5)) in Equations (1-2), a linear eigenvalue problem is obtained as follows:

$$\sigma[\,a,\,\alpha(U,P)]\mathcal{C}V_{lin}(a,z) = \{\mathcal{A} + \alpha(U,P)\,\mathcal{B}\}\;V_{lin}(a,z), \tag{6}$$

where V_{lin} indicates the linear vector fields. A detailed form of the linear eigenvalue problem can be rewritten as

$$\begin{aligned} \sigma \begin{pmatrix} \tilde{N}_e \\ \tilde{N}_i \\ \tilde{N}_a \end{pmatrix} &= D\left(\frac{1}{r}\frac{\partial}{\partial r} + \frac{\partial^2}{\partial r^2} - a^2\right) \begin{pmatrix} 1 & 0 & 0 \\ 0 & 1 & 0 \\ 0 & 0 & 1 \end{pmatrix} \begin{pmatrix} \tilde{N}_e \\ \tilde{N}_i \\ \tilde{N}_a \end{pmatrix} \\ &\quad + \alpha \begin{pmatrix} \tilde{N}_e \\ \tilde{N}_i \\ \tilde{N}_a \end{pmatrix}. \end{aligned} \tag{7}$$

In the case of Poisson's equation, Eq. (2) can be written as follows by the boundary conditions in Eq. (4):

$$\left(\frac{1}{r}\frac{\partial}{\partial r} + \frac{\partial^2}{\partial r^2} - a^2\right)\tilde{\phi} + \frac{4\pi}{\varepsilon}e\left(\tilde{N}_e - \tilde{N}_i\right) = 0. \tag{8}$$

The condition that the maximal real part of σ vanishes (*i.e.* $\Re\left[\sigma(\,a,\,\alpha(U,P))\right] = 0$), a neutral curve (*i.e.* linear stability curve in order to satisfy the conditions for the generation of a plasma pattern) is determined at U_c. The minimal value of U with respect to a yields the critical wave number a_c. Thus, the critical wave number a_c satisfies the critical voltage $U_c = U_0(a_c)$ for a given gas pressure. In order to gain more information about the concept of linear stability analysis, we refer to [20, 21].
In the literature, the empirical formula $\alpha(U,P)$ is frequently used to identify the relation between the voltage and pressure in the electrical discharge studies of various plasma systems [22, 23]. The explicit form of the α control parameter is a function of the voltage U and pressure P variables,

$$\alpha\,(U,P) = A\,P\,\exp\left(\frac{BPd}{U}\right), \tag{9}$$

depending on the geometry of the model. In Eq. (1), the source term Q^+ includes $\alpha(U,P)$ and defines a condition

for the generation of particles as stated before. This formula was empirically determined by Lozanckij *et al.* [24] and used in some previous studies such as [17, 22, 23]. Here P is the PF pressure in units of Pascals (Pa) and U is voltage in Volts. The radial distance between the anode and cathode is indicated by d and it has a value of $d = 2.5$ cm in our simulation. A and B are constants for given conditions and a more detailed determination of these empirical constants can be found in [25]. For this study, we use the values $A = 1$, $B = 1000$ and $B = 3000$ in our units. The drift velocity for electrons is given by $\vec{u_e} = \mu_e \nabla\phi$, however we do not take into account this term since it is not a linear one. The electron mobility $\mu_e = e/m_e\nu_{ea}$ consists of electron charge, electron mass and the electron-atom collision rate. In the physical frame, we assume that electrons are emitted from the cathode by the incidence of positive ions. The anode surface is assumed to be perfectly absorbing.

From the physical point of view, when a large voltage pulse between the electrodes is realized, this leads to acceleration of electrons at the end of ionization process. However it is important to obtain definite information on the starting point of the scenario which triggers the above-mentioned processes. It has been proven that it is possible to obtain analytical solutions of discharge breakdown models in cylindrical geometry for very low current densities [17]. In the case of higher voltages and currents, ionization coefficients render nonlinear equations and numerical procedures could be applied for a complete picture of the system. Even without the nonlinear terms, a numerical approach can give a more realistic description than analytical studies. In this framework some limited aspects of discharges were studied by [26] and it can not be generalized to a PF system. In addition, the authors assumed a parallel plane scheme in their model.

3. Results and discussion

The simulations are carried out for the inter-electrode area of a PF, which is sketched out in Fig. 1. The difference between the radius of the inner and outer electrodes are assumed to be $d = 0.025$ m. We assume any gas with varying pressures to determine the linear analysis for this study. However a special gas type can easily be adopted to the model depending on the material characteristics. In our study, the maximum charging voltage is considered to be $U = 16$ kV and a wide range of voltages and pressure values are investigated.

According to the simulations, the onset of breakdown is found to be oscillatory for all cases. Note that the oscillatory case is defined by $\Im[\sigma(a_c, \alpha(U_c, P))] \neq 0$. This kind of oscillatory result also supports the general view in which the plasma sheath is not stationary; in fact moving through the tip of the electrodes.

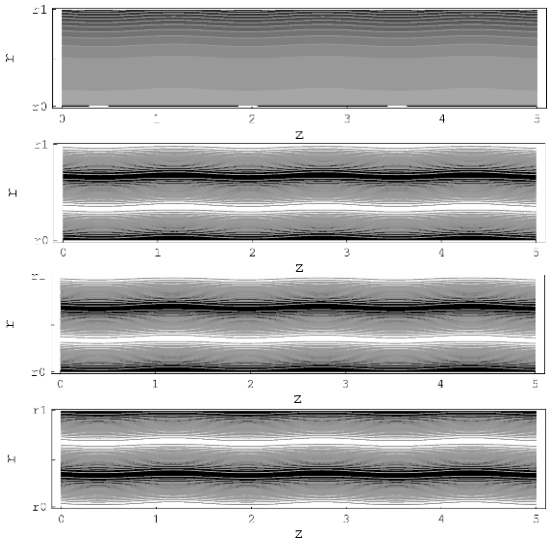

Figure 2. From top to bottom, contours of potential function, electron, ion and excited atom densities for diffusion coefficient $D = 1$, voltage $U = 7.727$ kV, wave number $a = 4.0$, $B = 1000$ and $P = 200$ Pa ($\Im(\sigma) = 0.013$). The contour values decrease from white to black color.

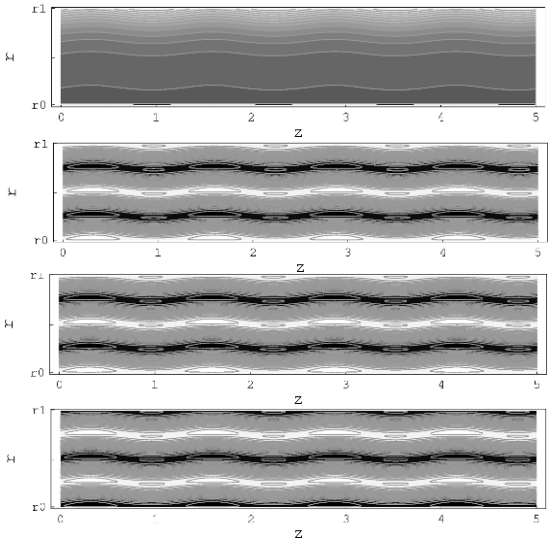

Figure 3. From top to bottom, contours of potential function, electron, ion and excited atom densities for diffusion coefficient $D = 10$, voltage $U = 5.285$ kV, wave number $a = 4.9$, $B = 1000$ and $P = 20$ Pa ($\Im(\sigma) = 0.103$). The contour values decrease from black to white color.

A series of two dimensional density and potential contours on $(r - z)$ plane are shown in Fig. 2. Note that the potential lines of the ϕ function are in the order of

kV. In the potential contour, there exist parallel constant potential lines which have lower values toward the outer electrode. A wavy appearance in the contours can be acceptable because of an oscillatory behavior of the plasma. We refer to [27] for the detailed dynamics of these contours in terms of tokamak plasma. For lower values of $\Im[\sigma]$, island-type particle densities which are found in the above reference can not be observed, however the particle densities become island-type when $\Im[\sigma] > 0.1$ is fulfilled (see, for instance, Fig. 3). The contours of the electron and ion densities are similar to each other, giving maximal values at $r = 1/3$ and $r = 1$. Contours of densities are seen parallel to constant potential lines. The position of maximal and minimal contour lines of N_e and N_i are similar to each other. Whereas the positions of maximal and minimal densities of N_a are different from those of N_e and N_i (i.e maximal density values of N_a contour plot are at $r = 0$ and $r = 2/3$).

In the case of a relatively higher diffusion coefficient, $D = 10$, we show the same type of plot (Fig. 3). The particle densities with island-types are observable for this parameter set. Note that the island-type densities and potential contours can be clearly obtained for the pressure and voltage values (P, U) which are higher then the critical values (P_c, U_c). In other words, the higher are the $(P - P_c, U - U_c)$ values, the higher are the imaginary part of the growth rates. It is easy to define the distance to those critical values for a given parameter set by using a linear analysis. One contribution of this study is to construct the linear stability regions in terms of parameter sets. For the case in Fig. 3, $\Im(\sigma) = 0.103$ is obtained for those parameters. Wavy potential lines and islands are clearly seen in this figure. Note also that the density contours of the particles also change dramatically since the local higher and lower contours differ from the case in Fig. 2. Asymmetry between electron and excited atom densities are preserved as well.

Fig. 3 also gives interesting information on the spatial distribution of particles in the sense that the densities indicate maxima and repeat themselves along the $z-$ axis (*i.e.* anode). Such kind of behavior has also been obtained in a recent numerical study of Yordanov *et al.* [4]. In their Monte-Carlo simulations, they have found that the electron densities in the inter-electrode area of a PF give a number of maxima along the inter-electrodic space in the breakdown and post-breakdown (axial) phases.

The linear thresholds are shown in Fig. 4a. We find two representative curves for two different B parameters, namely $B = 1000$ (bottom) and $B = 3000$ (top). Note that B is one of the constants under the given conditions and it can be empirically determined for a PF. It is clear that the threshold increases dramatically by increasing B as seen

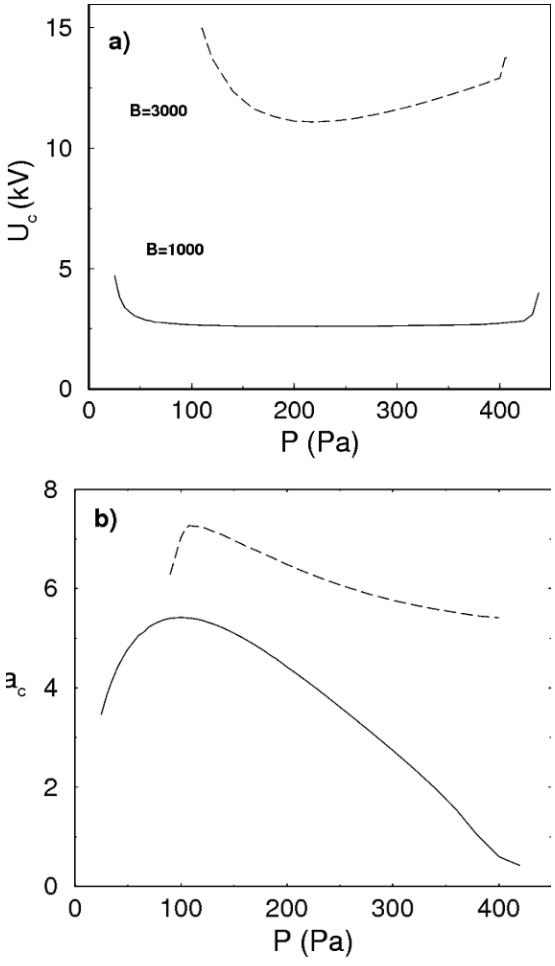

Figure 4. (a) The variation of the critical voltage U_c as a function of the PF pressure P (i.e stability curve) in the cases $B = 3000$(top) and $B = 1000$(bottom). (b) The corresponding critical wave number a_c for the plasma pattern as a function of pressure P in the cases of same B notation. $D = 1$ for both of the graphs.

in Fig. 4a. Another point is that the linear threshold curve becomes narrow when B becomes higher. Strictly speaking, the minimal points of these two curves correspond to the pressure values of $P = 200$ Pa and $P = 220$ Pa for the upper and lower curves, respectively. For a more detailed picture, see Table 1.

The corresponding critical wave numbers (a_c) as function of PF pressures are represented in Fig. 4b. Trends of these curves are similar to each other for different values of B, however the wave numbers become higher when the B parameter increases. For the lower pressures, a_c starts to increase up to a maximum value. At a moderate pressure

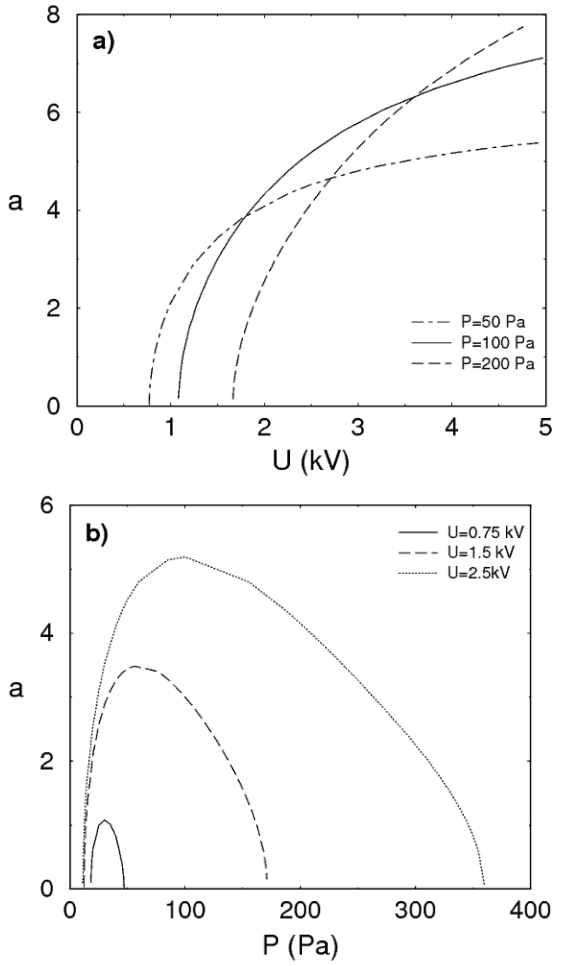

Figure 5. (a) Variation of the wave number a as a function of initial voltage U in the cases $P = 50$ Pa, 100 Pa and 200 Pa. (b) Variation of the wave number a as a function of the PF pressure P in the cases $U = 0.75$ kV, 1.5 kV and 2.5 kV. Diffusion coefficient is $D = 1$.

of PF, it gives a maximal value, then it starts to decrease for higher pressures as in Fig. 4b.

Apart from aforementioned critical values, we also look for the variation of the pattern wave number a as a function of initial voltage U. Such a graph is given in Fig. 5a for various values of gas pressure. It is clear from the graph that there exists no solution below a certain voltage value for each pressure rate. It is reasonable in the sense that the formation of plasma in the inter-electrode space can not be observed for every U voltage value. Furthermore when the pressure of the system is increased, one needs higher voltages in order to form a plasma pattern. Note also that the relation of voltage and wave number indicates a parabolic shape for increasing pressure (*i.e.* $U \propto a^2$).

In Fig. 5b, the variation of wave number as function of pressure is shown for various U values. The variation of a is noteworthy since it determines a pressure range for certain U initial voltages. In other words, a PF can work under a certain range of pressure values. This pressure range is, for instance, between $20 - 48$ Pa for the voltage of $U = 0.75$ kV. However, when the voltage increases, the usable pressure range also gets larger as seen for $U = 2.5$ kV. According to this result, it can be stated that if one wishes to work at a large pressure interval, in this case higher voltages should be applied to a PF.

Table 1. Some critical parameters for the formation of plasma pattern. Diffusion coefficient is $D = 1$.

Pressure (Pa)	$B = 1000$		Pressure (Pa)	$B = 3000$	
	U_c (kV)	a_c		U_c (kV)	a_c
25	4.699	3.468	110	14.975	7.317
100	2.670	5.417	140	12.368	7.073
200	2.609	4.422	220	11.084	6.307
340	2.652	1.976	300	11.595	5.764
400	2.732	0.602	400	12.909	5.411

4. Concluding remarks

The linear stability of a PF system is investigated theoretically in a 2-D framework. It is found that the linear threshold for the plasma formation between the electrodes of such a device is sensitive to initial parameters such as the voltage, pressure and structural constants. The pattern characteristics are considered by means of the wave number which is found to be dependent on the pressure, applied voltage and structural constants. Depending on the structural constants, the threshold for critical voltage changes from the order of $U_c = 2.5$ kV to $U_c = 11$ kV by increasing B. In addition, the wave number of the pattern determines certain pressure intervals for any given voltage U. We suggest that our model can be applied to any PF device in order to optimize them. Strictly speaking, one should adjust the appropriate initial voltage depending on the pressure intervals for experiments in order to observe an accelerated plasma pattern.

References

[1] J.H. Lee, D.R. McFarland, W.L. Harries, Plasma Physics 20, 1025 (1978)

[2] H. Herold, A. Jerzykiewicz, M. Sadowski, H. Schmidt, Nucl. Fusion 29, 1255 (1989)

[3] M.J. Sadowski, M. Scholz, Plasma Sources Sci. T. 17, 1 (2008)
[4] V. Yordanov, D. Genov, I. Ivanova-Stanik, A. Blagoev, Vacuum 76, 365 (2004)
[5] H.M. Soliman, M.M. Masoud, Phys. Scr. 50, 406 (1994)
[6] M. Borowiecki et al., Czech. J. Phys. 56, 184 (2006)
[7] J. Feugeas, O. von Pamel, J. Appl. Phys. 66, 1080 (1989)
[8] H. Krompholz, W. Neff, F. Ruhl, K. Schonbach, G. Herziger, Phys. Lett. A 77, 246 (1980)
[9] A. Donges, G. Herziger, H. Krompholz, F. Ruhl, K. Schonbach, Phys. Lett. A 76, 391 (1980)
[10] M. Borowiecki et al., In: 4th International Workshop on Plasma Physics and Z-pinch Research, Sep. 1985, Warsaw, Poland (Institute of Plasma Physics and Laser Microfusion) 86
[11] W. Stepniewski, Vacuum 76, 51 (2004)
[12] S. Lee, C.S. Wong, T.Y. Tou, In: S. Lee et al. (Ed.), Proceedings of 1st Tropical College on Applied Phys: Laser and Plasma Technology, 26 Dec. 1983 - 14 Jan. 1984, Kuala Lumpur, Malaysia (World Scientific) 1
[13] M.M. Mesoud, H.A. El-Gamal, H.A. El-Tayeb, M.A. Hassouba, M.A. Abd Al-Halim, Plasma Dev. Oper. 15, 263 (2007)
[14] H. Bhuyan, S.R. Mohanty, N.K. Neog, S. Bujarbarua, R.K. Rout, Meas. Sci. Technol. 14, 1769 (2003)
[15] T.Y. Tou, IEEE Trans. Plasma Sci. 23, 870 (1995)
[16] S.P. Chow, S. Lee, B.C. Tan, J. Plasma Phys. 8, 21 (1972)
[17] M. Scholz, I.M. Ivanova-Stanik, Vacuum 58, 287 (2000)
[18] B.E. Keen, W.H.W. Fletcher, J. Phys. D Appl. Phys. 3, 1868 (1970)
[19] M. Momeni, I. Kourakis, M. Moslehi-Fard, P.K. Shukla, J. Phys. A Math. Theor. 40, 473 (2007)
[20] E. Kurt, F.H. Busse, W. Pesch, Theo. Comp. Fluid Dyn. 18, 251 (2004)
[21] F.H. Busse, In: W. Peltier (Ed.), Mantle convection, plate tectonics and global dynamics (Gordon and Breach, New York, 1989) 35
[22] Y.P. Rayzer, Gas Discharge Physics (Springer, Berlin, 1991)
[23] H.Y. Kurt, B.G. Salamov, J. Phys. D Appl. Phys. 36, 1987 (2003)
[24] E.D. Lozanckij, O.B. Firsov, Teorija iskry (Moskva Atomizdat, 1975) 106 (in Russian)
[25] K.T.A.L. Burm, Contrib. Plasma Phys. 47, 177 (2007)
[26] A.J. Davies, C.J. Evans, P. Townsend, P.M. Woodison, IEEE Proc. 124, 179 (1977)
[27] R. Fitzpatrick, F.L. Waelbroeck, F. Militello, Phys. Plasmas 13, 1 (2006)